Article

Detection of Uracil-Excising DNA Glycosylases in Cancer Cell Samples Using a Three-Dimensional DNAzyme Walker

Jeffrey Tao, Hongquan Zhang,* Michael Weinfeld, and X. Chris Le*

Cite This: *ACS Meas. Sci. Au* 2024, 4, 459−466

Read Online

ACCESS | 📊 Metrics & More | 📖 Article Recommendations | 🔘 Supporting Information

ABSTRACT: DNA glycosylase dysregulation is implicated in carcinogenesis and therapeutic resistance of cancers. Thus, various DNA-based detection platforms have been developed by leveraging the base excision activity of DNA glycosylases. However, the efficacy of DNA-based methods is hampered due to nonspecific degradation by nucleases commonly present in cancer cells and during preparations of cell lysates. In this report, we describe a fluorescence-based assay using a specific and nuclease-resistant three-dimensional DNAzyme walker to investigate the activity of DNA glycosylases from cancer cell lysates. We focus on DNA glycosylases that excise uracil from deoxyuridine (dU) lesions, namely, uracil DNA glycosylase (UDG) and single-stranded monofunctional uracil DNA glycosylase (SMUG1). The limits of detection for detecting UDG and SMUG1 in the buffer were 3.2 and 3.0 pM, respectively. The DNAzyme walker detected uracil excision activity in diluted cancer cell lysate from as few as 48 A549 cells. The results of the UDG inhibitor experiments demonstrate that UDG is the predominant uracil-excising glycosylase in A549 cells. Approximately 500 nM of UDG is present in each A549 cell on average. No fluorescence was generated in the samples lacking DNAzyme activation, indicating that there was no nonspecific nuclease interference. The ability of the DNAzyme walker to respond to glycosylase activity illustrates the potential use of DNAzyme walker technology to monitor and study biochemical processes involving glycosylases.

KEYWORDS: DNAzyme, uracil DNA glycosylase, base excision repair, UDG, SMUG1, biosensors
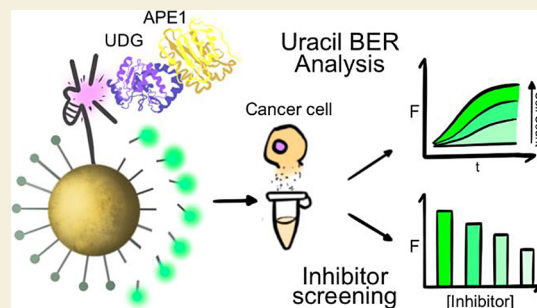
DNA repair enzymes have sparked clinical interest as biomarkers and therapeutic targets because of their role in the initiation and progression of disease. Base excision repair (BER) is initiated by DNA glycosylases that recognize and excise oxidized, alkylated, or deaminated bases. Altered DNA glycosylase activity, often arising from single nucleotide polymorphisms (SNPs) that repress activity, is implicated in the development of metabolic disorders and the onset of carcinogenesis because of the accumulation of damaged DNA, gene mutations, and deregulated DNA repair mechanisms.[1−4] As cancers progress into more genomically hostile conditions because of reactive oxygen species (ROS) and widespread DNA damage, cancer cells adapt by overexpressing DNA glycosylases and other BER enzymes. The overexpression of DNA glycosylases in advanced-stage cancers also confers resistance to chemo- and radiotherapies that act by inducing DNA damage to eliminate cancer cells.[5−8] Therefore, efforts are being invested into the identification of glycosylase inhibitors with the goal of sensitizing advanced tumors to anticancer therapies.[6,9−11]

The link between DNA glycosylases and disease spurred the development of assays for these enzymes and their activities. These methods used simple DNA substrates labeled with fluorophores,[12] radioisotopes,[13,14] and chemiluminescent molecules.[15] More recent examples of glycosylase assays incorporate DNA amplification techniques[16,17] and signal amplification techniques using DNAzymes[18,19] and CRISPR-Cas trans-cleavage.[20] Although sensitive, DNA amplification techniques are complicated and time-consuming, involving multiple technical steps and incubation periods. DNA-amplification techniques can detect intracellular glycosylases after their introduction into the cell by lipofectamine transfection or MnO_2 nanosheets,[21−23] but the engulfed DNA is prone to nuclease digestion, which risks false positive results or attenuates detection altogether. Furthermore, lipofectamine is limited to in vitro applications.
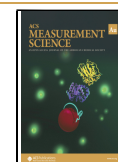
DNAzyme walkers functionalized on gold nanoparticles (AuNPs) have the potential to overcome the aforementioned limitations. The spherical DNA conjugated onto AuNPs forms a negatively charged barrier that inhibits nucleases from digesting the DNA.[23,24] Furthermore, spherical nucleic acids are readily endocytosed into cancer cells.[25−29] We previously

demonstrated the capacity of DNAzyme walkers to target BER enzymes by detecting APE1 in living cancer cells.[30] We therefore sought to expand the application of our DNAzyme walker to investigate DNA glycosylase activity in cancer cell samples. There are 11 known DNA glycosylases in human cells, each specific for different base lesions. When targeted by a DNA glycosylase, the damaged base is flipped out of the DNA helix and into the glycosylase activity site to cleave the N'-glycosidic bond.[31,32] We focused on targeting uracil DNA glycosylase (UDG or UNG) and single-strand-selective monofunctional uracil DNA glycosylase (SMUG1). Other DNA glycosylases, such as 8-oxoguanine DNA glycosylase (OGG1) and alkyladenine DNA glycosylase (AAG), are also well characterized and remain potential targets for investigation using the DNAzyme walker.

UNG is the major UDG involved in the excision of uracil from deoxyuridine (dU) lesions, while SMUG1 is considered a backup uracil glycosylase with a broader range of substrates including methylated and oxidized dU.[33−35] In humans, hUNG2 and hSMUG1 are localized in the nucleus, while hUNG1 is expressed within the mitochondria.[36] In HeLa cells, SMUG1 is abundantly present in the cytoplasm, which is characteristic of cancer pathology.[34] Both UNG and SMUG1 target dU in ssDNA and dsDNA, though they demonstrate a preference for ssDNA.[33,34,37] Uracil lesions in DNA arise from spontaneous cytosine deamination and dUTP-mediated misincorporation during DNA replication, risking mutagenic transit from C:G to T:A base pairs within genes.[38] UNG and SMUG1 are the most well-characterized glycosylases with respect to crystal structure, specificity, catalytic efficiency, and cellular localization.[34,36,39−42] To evaluate the design of the DNAzyme walker, we used *E. coli* UDG, which is comparable to human UNG in its folded structure and function.[32,34,43,44] We then applied the DNAzyme walker to assess UDG and SMUG1 activity from A549 cancer cell samples.

Despite sharing the N'-glycosylase activity, each of the DNA glycosylases is different in binding and kinetic properties and non-BER functions in cancer cells. Therefore, UDG and SMUG1 were expected to interact with our DNAzyme walker system with appreciable differences that we elucidate in this report.

■ EXPERIMENTAL SECTION

Chemicals and Reagents

Oligonucleotides were purchased from Integrated DNA Technologies (IDT, Coralville, IA), and their sequences are shown in Table S2. AuNPs, 20 nm in size, were purchased from Ted Pella (Redding, CA). APE1, UDG (uracil DNA glycosylase), SMUG1 (single-strand selective monofunctional uracil DNA glycosylase 1), EndoIV (endonuclease IV), AAG (alkyl adenine DNA glycosylase), Fpg (formamidopyrimidine DNA glycosylase), UGI (uracil DNA glycosylase inhibitor), and BSA (bovine serum albumin) were purchased from New England Biolabs (NEB, Whitby, ON, Canada). IgG from human serum and $MnCl_2$ solution were purchased from MilliporeSigma (Oakville, ON, Canada). HeLa cells were propagated from cryopreserved cell lines purchased from the American Type Culture Collection (Manassas, VA). Acrylamide/bis-acrylamide solution (40%) (39:1) was purchased from BioRad (Hercules, CA). NaCl, $MgCl_2$, KCl, EDTA, Tris-HCl, Tris-acetate, trypsin, Tween-80, Tween-20, Triton X-100, and DNA Gel Loading Dye (6×) were purchased from Thermo Fisher Scientific (Mississauga, ON, Canada).

Construction of the DNAzyme Walker

The DNAzyme was first hybridized with the blocker strand using a BioRad T100 thermocycler (Hercules, CA) set to decrease 0.1 °C every 5 s, starting from 80 °C and ending at 20 °C. The blocked DNAzyme and carboxyfluorescein (FAM)-labeled oligonucleotide track strands were then mixed with 1 mL of 20 nm AuNPs (7×10^{11} particles/mL) that was premixed with 0.625% Tween-80. The molar ratio of blocked DNAzyme to FAM-labeled track strands was 200:1000 per AuNP. Forty microliters of 5 M NaCl was added to the DNA/AuNP mixture every 30 min five times for a final concentration of 0.83 M NaCl. After overnight maintenance at room temperature in the dark, the salted AuNPs were subjected to centrifugation at 17,500×g. The supernatant was collected and discarded, carefully leaving the pellet undisturbed. DNA-AuNPs were washed with wash buffer (100 mM NaCl, 10 mM Tris-HCl (pH 7.4), 0.05% Tween-20) and centrifuged at 21,100×g for 20 min, then the supernatant was removed. The wash step was repeated twice more. Finally, the AuNPs functionalized with the DNAzyme walker were stored in 0.5 mL of storage buffer (200 mM NaCl, 10 mM Tris-HCl (pH 7.4), 0.05% Tween-20) at 4 °C until use.

Determination of DNA Glycosylases in Buffer

Each 100 μL reaction volume contained 230 pM AuNPs functionalized with the DNAzyme walker, 50 nM NaCl, 50 mM KCl, 20 mM Tris-acetate (pH 7.9), 3 mM $MgCl_2$, 500 μM $MnCl_2$, 0.1 U APE1 and varying concentrations of UDG and SMUG1. $MgCl_2$ and $MnCl_2$ were added as the final step before recording fluorescence at 25 °C using the fluorometer. Samples containing Fpg did not contain APE1 because of the dual glycosylase/AP lyase activity of Fpg but consisted of the same reaction mixture. Specificity tests were conducted using the same reaction buffer and 0.1 U of APE1, UDG, Fpg, EndoIV, and hAAG, and 30 μM BSA and 33 μM IgG. Unit definitions for enzymes are shown in Table S1.

Incubation, Collection, and Lysis of A549 Cells

A549 cells were cultured in Dulbecco's modified essential medium (DMEM, Thermo Fisher Scientific) in a humidified incubator at 37 °C with 5% CO_2. Cells were grown to 85% confluency and then washed with 1X DPBS (Thermo Fisher Scientific) twice. Trypsin (0.25%) was added for 1 min to detach the cells, which were collected in the DMEM medium. The collected cells were centrifuged at 1000×g for 3 min, and the supernatant was aspirated to remove residual trypsin. The pelleted cells were dispersed with DMEM and cells were then counted using a hemocytometer.

For lysis, 10^6 cells were collected and washed with ice-cold 1X DPBS twice; 200 μL of ice-cold lysis buffer (1% TritonX-100, 150 mM NaCl, 50 mM Tris-HCl (7.4), 1 mM EDTA) was then added to the pellet, and the dispersed cells were pipetted up and down 10 times. The cells in the lysis buffer were left on ice for 20 min before centrifugation at 13,000×g for 30 min at 4 °C. The supernatant was then collected and diluted in lysis buffer without EDTA for a final concentration equivalent to the cell contents of 10000 cells/μL. Serial dilutions were carried out using lysis buffer without EDTA. Unused samples were flash-frozen and stored at −80 °C until future use.

■ RESULTS AND DISCUSSION

Principle and Design of the DNAzyme Walker for the Detection of Glycosylases

The operation of the DNAzyme walker is displayed in Scheme 1. The DNAzyme walker was modified from the design for the detection of the AP site that we previously published[30] by taking into account the reaction of glycosylases upstream to the formation of the AP site.[30] We incorporated the dU in the middle of the blocker to tailor the DNAzyme for UDG/SMUG1 detection (Table S2 and Figure S1). The glycosylases cleave uracil from the bound blocker to form a natural AP site (Scheme 1). After the incision of the AP site, the cleaved blocker then separates into weakly hybridized fragments that dissociate from the DNAzyme. The activated DNAzyme is then free to bind and cleave the conjugated track strands to amplify the fluorescence. In the absence of the target UDG/

Scheme 1. DNA Glycosylase Detection with the DNAzyme Walker[a]
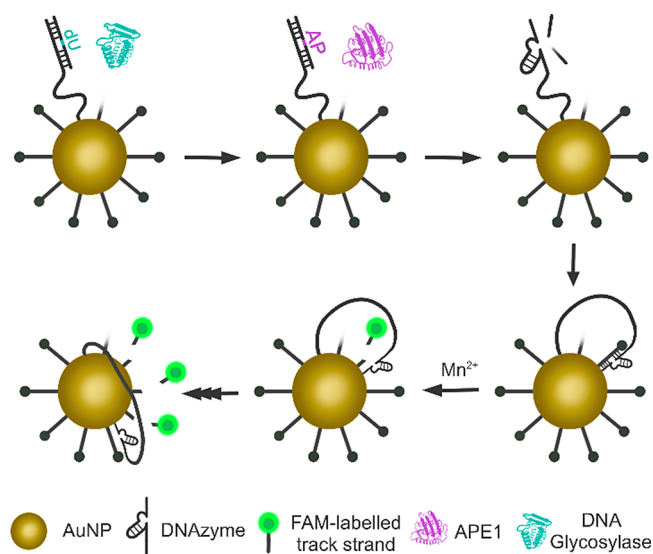
[a]UDG and SMUG1 identify and cleave dU within the blocker DNA. The leftover AP site is then processed by APE1, cleaving the blocker DNA. The blocker DNA fragments dissociate from the DNAzyme, allowing the DNAzyme to bind to track strands. In the presence of Mn^{2+} cofactor, the DNAzyme is activated and the track strands are cleaved, evoking an amplified fluorescence signal in response to a single DNA glycosylase-catalyzed reaction.

SMUG1, the blocking strand remains hybridized to the DNAzyme and the DNAzyme is inactive, thus no fluorescence is generated.

The activation of the DNAzyme walker involves both DNA glycosylase activity and the cleavage of the AP site. Thus, the activities of UDG and SMUG1, along with the cleavage of the AP site by APE1 lyase activity, are necessary for the generation of fluorescence by the DNAzyme walker.[45,46] APE1 is known to coordinate with DNA glycosylases and stimulate glycosylase activity.[34,47−50] Furthermore, glycosylases within cancer cells likely have highly varying activities because of the plethora of proteins and pathways that interact with the glycosylases. Therefore, the DNAzyme-mediated responses reported here should be understood to result not only from base excision but also from a dynamic coordination between the glycosylases, APE1, and other factors in cancer cells. Among the DNA glycosylases studied, only Fpg has both glycosylase and lyase activity. Fpg does not require APE1 to activate the DNAzyme walker.

Examining UDG and SMUG1 Activity in Buffer

The DNAzyme walker adapted with the dU blocker (dU-DNAzyme walker) elicited a concentration-dependent fluorescence in response to UDG and SMUG1 (Figure 1). The limit of detection (LOD) for UDG detection was 3.2 pM (0.97 mU, unit definitions provided in Table S1) with a linear range between 3.3 and 67 pM (0.001−0.02 U) (Figure 1A), while the LOD for SMUG1 detection was 3.0 pM (4.5 mU) with a linear range of 6.7−67 pM (0.01−0.1 U) (Figure 1B). The high sensitivity may be partially attributed to the design of the system. The dU lesion is adjacent to a G and C residue and is amidst a broader GC-rich region, which is a preferred substrate of UDG.[51,52]

We hypothesized that the dU-DNAzyme walker would be more sensitive for UDG than SMUG1 because hUNG2, the human equivalent UDG, is more catalytically efficient in cleaving dU from dsDNA.[34,53,54] The unit definitions also suggest that the *E. coli* UDG is much more active in cleaving uracil than SMUG1 per mol/U (Table S1). However, the DNAzyme walker responded to similar concentrations of both UDG and SMUG1. Fluorescence trends for SMUG1 detection also required only half the time as the UDG trends before reaching a plateau, suggesting a more robust activation of the DNAzyme walker by SMUG1 than UDG (Figure 1B). These unexpected findings may be because the UDG tested here is of the *E. coli* enzyme, which likely does not coordinate with human APE1 to the same degree as human SMUG1.[34] Nonetheless, the sensitivity for the dU-excising glycosylases was about 20 times less than for the DNAzyme walker tailored for APE1 detection.[30] The lower sensitivity is reasonable considering that two enzyme-catalyzed reactions are required for the activation of the DNAzyme to detect monofunctional glycosylases with the DNAzyme walker.

The dU-DNAzyme walker-mediated fluorescence was specific to UDG and SMUG1 in comparison to other glycosylases and proteins (Figure 1C). Without APE1 or Mn^{2+}, only background fluorescence was generated (Figure 1C). Furthermore, uracil DNA glycosylase inhibitor (UGI) inhibited UDG activity and diminished fluorescence generation in a concentration-dependent manner (Figure 1D). UGI irreversibly binds and inhibits UDG with 1:1 stoichiometry,[55,56] which is evident by the background fluorescence levels observed when 0.1 U of both UDG and UGI are present (Figure 1D). Both UDG and APE1 are functional between room temperature and 37 °C,[34,40,43,57] and we found 25 °C to be optimal for UDG detection with the DNAzyme walker (Figure S2). The ability of the dU-DNAzyme walker to detect BER enzymes at room temperature enables the application of our design for point-of-care testing without the need for heating.

Dissociation of the blocker from the DNAzyme is demonstrated by the PAGE gel shown in Figure 1E (lane 8). The DNAzyme-only lane contains two bands (lane 1); both bands respond similarly to the experimental conditions and so do not affect the qualitative analysis of the blocker dissociation. With only APE1, the blocked DNAzyme band remains intact despite the addition of Mg^{2+}, indicating that an active APE1 is unable to dissociate the blocker (Figure 1E, lane 4). In the presence of UDG, APE1, and Mg^{2+}, the blocker is successfully dissociated from the DNAzyme (Figure 1E, lane 8). Interestingly, an intermediary band forms between the free DNAzyme band and blocked DNAzyme band in the presence of UDG when APE1 and Mg^{2+} are not present (Figure 1E, lanes 5−7). The intermediary band cannot be explained by the binding of UDG to the blocked DNAzyme, since a protein−DNA complex would decrease band migration. We considered that the intermediary band could represent a blocked DNAzyme with an AP site after uracil excision. Although the intermediary band forms when Mg^{2+} is chelated (Figure 1E, lane 7), UDG is still catalytically active without Mg^{2+} and could excise uracil.[34] The chelated Mg^{2+} would only hinder APE1 activity and prevent the cleavage of the AP site after uracil excision, which is why blocker dissociation was not observed with APE1 and EDTA (Figure 1E, lane 7). However, additional PAGE analysis shows no difference in band patterns between the UDG-treated blocked DNAzymes with either a
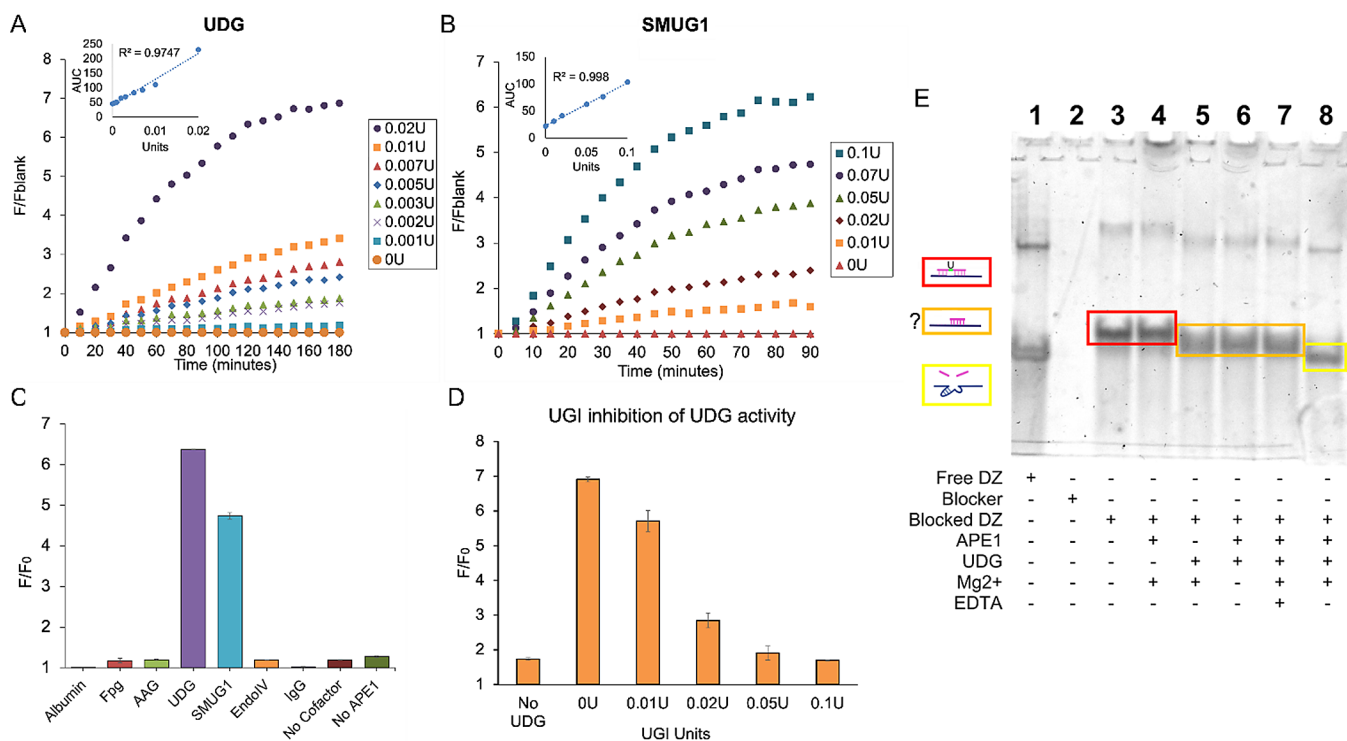
Figure 1. DU-DNAzyme walker is activated by UDG and SMUG1. (A) Detection of pure UDG in buffer. (B) Detection of pure SMUG1. (C) Selectivity of the dU-DNAzyme walker for UDG and SMUG1. The concentration of each enzyme was 0.1 U/100 μL. The concentration of BSA tested was 30 μM and IgG was 33 μM. Fluorescence was recorded after 60 min. (D) Uracil DNA glycosylase inhibitor (UGI) inhibits UDG activity and diminishes DNAzyme activation. Fluorescence was recorded after 90 min. Each sample, except for the "No UDG" control, contained 0.1 U of UDG. The "No UDG" control contained 0.1 U of UGI. (E) UDG activity appears to excise uracil, while APE1 and UDG activity dissociates the blocker from the DNAzyme, as visualized with the 10% native PAGE gel. The intermediary band outlined in orange is an unknown structure between the blocked (red) and liberated (yellow) DNAzyme bands. Each reaction mixture contained 50 nM NaCl, 50 mM KCl, 20 mM Tris-acetate (pH 7.9), and the following components: Lane 1, DNAzyme; lane 2, dU blocker; lane 3, blocked DNAzyme; lane 4, blocked DNAzyme + 0.1 U APE1 + 3 mM MgCl$_2$; lane 5, blocked DNAzyme + 0.1 U UDG + 3 mM MgCl$_2$; lane 6, blocked DNAzyme + 0.1 U UDG + 0.1 U APE1 without Mg^{2+}; lane 7, blocked DNAzyme + 0.1 U UDG + 0.1 U APE1 + 3 mM MgCl$_2$ + 10 mM EDTA; and lane 8, blocked DNAzyme +0.1 U UDG + 0.1 U APE1 + 3 mM MgCl$_2$. DZ: DNAzyme. Error bars represent one standard deviation from triplicate experiments.

dU or an AP lesion (Figure S3). Another possibility is that the intermediary band represents a fragment of the blocker DNA that is still bound to the DNAzyme, which would have a molecular weight between the free and fully bound DNAzyme bands. Human UDG was recently found to have a minor Mg^{2+}-independent lyase function[58] which may generate a different band pattern than the blocked DNAzymes cleaved by APE1. Despite the unknown cause of the intermediary band, it is evident that the free DNAzyme band is recovered when UDG, APE1, and Mg^{2+} are present, which indicates the successful dissociation of the blocker (Figure 1E, lane 8).

Detection of Uracil-Excising DNA Glycosylases in Diluted Cancer Cell Lysate

The DNAzyme walker induced higher overall fluorescence levels with increasing concentrations of diluted lysate of A549 cells. An LOD of 48 A549 cells and a linear range of 100−2000 cells was achieved (Figure 2A). Without metal cofactor, there was only background fluorescence, indicating that there was no nonspecific nuclease interference (Figure 2A). Endogenous APE1 levels were sufficient to process the AP site after uracil cleavage. The dU-DNAzyme walker had a sensitivity for dU-excising glycosylases from A549 lysate that was about 4−5 times less than the sensitivity of the DNAzyme walker for the detection of APE1, which had an LOD of 10 A549 cells and a linear range between 10 and 500 cells (Figure S4). The lower sensitivity is likely due to the requirement of two enzymatic

steps for DNAzyme activation. We attribute the fluorescence response to UDG > SMUG1 based on their reported activities in human cells.[34,59] Thymine DNA glycosylase (TDG), which also excises dU from mismatched base pairs, may contribute to DNAzyme activation, though to a lesser extent due to its much lower catalytic efficiency.[60]

Determination of the Proportion and Concentration of Uracil-Excising Glycosylases in A549 Cells

We then determined what proportion of the fluorescence generated in diluted A549 lysate was due to UDG activity by adding varying amounts of uracil DNA glycosylase inhibitor (UGI). Fluorescence levels decreased with increasing concentrations of UGI (Figure 2B). With saturating levels of UGI (0.005 U), the fluorescence response decreased to near background levels (Figure 2B). To propose that UDG is primarily responsible for the activity inhibited by UGI, we must be sure that UGI specifically inhibits UDG and not SMUG1 or TDG. Early reports demonstrate strong inhibition of human and *E. coli* UDG[55,56,61,62] and a lack of inhibition of TDG by UGI[63] but the inhibition of SMUG1 by UGI is less clear. Reports that show SMUG1 to be UGI-resistant are based on qualitative PAGE analysis[53,63] which cannot determine whether SMUG1 is completely or partially resistant to UGI. Another report claims that ~40% of SMUG1 activity was inhibited by UGI,[34] although data were not shown. Therefore, we tested whether SMUG1 could be inhibited by UGI.
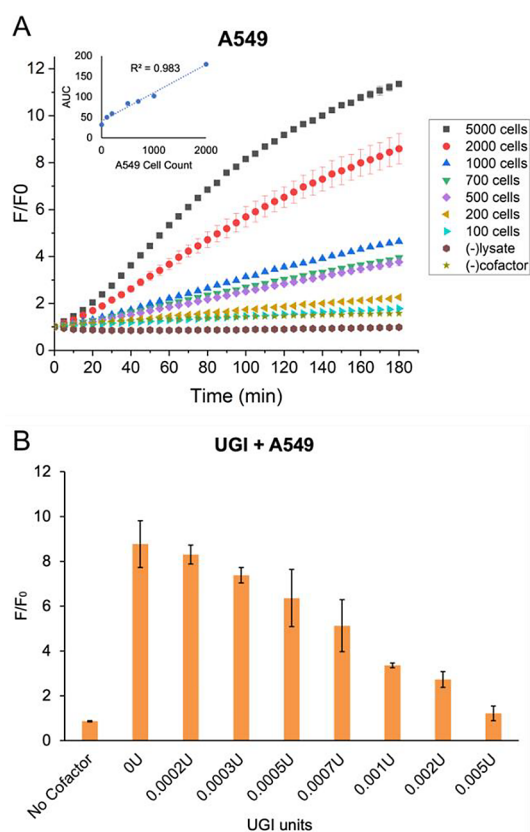
Figure 2. Glycosylases that excise dU were detected in the lysate of A549 cancer cells. (A) A549 cell count dependence on overall fluorescence increase over time and (B) UGI inhibits UDG and diminishes the fluorescence response. Each sample contained diluted cancer cell lysate equivalent to 2000 A549 cells. Fluorescence was recorded after 3 h. Error bars represent one standard deviation from triplicate experiments.

Interestingly, for the upper limit of SMUG1 detection at 0.1 U, 0.007 U of UGI was enough to decrease the fluorescence response by nearly 40% (Figure S5). With increasing concentrations of UGI beyond 0.01 U, we observed less inhibition of SMUG1 activity (Figure S5). We considered this may be due to increasing levels of DTT from the stock solution of UGI as we added more units into each sample, but our control tests show that even 1 mM DTT was unable to significantly detach the track strands from the AuNP surface (Figure S6). Although SMUG1 can be inhibited by UGI (Figure S5), the loss of almost all the fluorescence signals in the A549 lysate samples with saturating levels of UGI must predominantly result from UDG inhibition (Figure 2B). If SMUG1 contributed a significant proportion of DNAzyme activation, then we would expect 0.005 U of UGI to show only partial inhibition of fluorescence generation (up to ~40%), but this was not observed. Other reports show that UDG in HeLa cells contributes >98% of dU-excising activity[34,37] and that A549 cells show substantial overexpression of UDG[64] which further supports that the fluorescence observed in the diluted A549 lysate primarily results from UDG activity. Furthermore, our results demonstrate the ability of our DNAzyme walker to screen for UDG inhibitor activity in cancer cell samples.

For the following estimation of the amount of UDG in each A549 cell, we assume that all the fluorescence results from UDG activity and that *E. coli* and human UDG share unit definitions. Both UDGs are completely inhibited at similar concentrations of saturating levels of UGI.[61] If a 1:1 ratio of UDG units to UGI units abolishes the fluorescence response observed in the buffer studies (Figure 1D), and 0.005 U of UGI is required to diminish the fluorescence response in the diluted lysate of 2000 A549 cells (Figure 2B), then we estimate that there is approximately 2.5 μU, or 21.5 fg (calculated from parameters listed in Table S1), of UDG in each A549 cell. If the molecular weight of UDG is 25.7 kDa and the cell volume of an A549 cell is 1670 μm^3 (or 1.67 pL),[65] then the concentration of UDG per A549 cell is ~500 nM on average.

CONCLUSIONS

We successfully demonstrated the application of DNAzyme walkers for the investigation of uracil excision activity by UDG and SMUG1 in buffer and A549 cell lysate. Upon the excision of a damaged base and subsequent cleavage of the remaining AP site within the blocker, the DNAzyme binds and cleaves a track of FAM-labeled strands conjugated onto 20 nm diameter AuNPs to generate a concentration-dependent fluorescence response. The sensitivity of the DNAzyme walker was comparable to those of other UDG assays, including assays with DNA amplification steps (Table S3). We demonstrate that endogenous APE1 is sufficient for the detection of UDG in cell lysates, whereas other assays often require the addition of high amounts of either APE1 or Endo IV (Table S3). Finally, our method was able to measure UDG activity in cell lysate without the need for DNA amplification or heating steps.

Our technique has the potential to operate within live cells, where the real-time effectiveness of glycosylase inhibitors or chemotherapy sensitizers can be monitored.[6,9] However, the sequestration of the DNAzyme walker in endosomes may limit intracellular glycosylase detection.[66] Immune cells and hepatic clearance may also prevent the DNAzyme walker from accessing cancerous sites in vivo.[67] Future work could extend the DNAzyme walker technology to studies of a variety of DNA glycosylases, in addition to UDG and SMUG1, from cancer cells. The detection of glycosylase activity in more complex samples is yet to be realized.

ASSOCIATED CONTENT

Supporting Information

The Supporting Information is available free of charge at https://pubs.acs.org/doi/10.1021/acsmeasuresciau.4c00011.

> Details of the unit definitions and parameters for each NEB enzyme; details of the oligonucleotide sequences; various UDG assays with our DNAzyme walker; schematic details of the operating DNAzyme walker; temperature dependence for the detection of UDG; additional PAGE gels showing blocker strand displacement; detection of APE1 in A549 lysate using a DNAzyme walker adapted with a blocker with an AP site; UGI inhibition of SMUG1-mediated activation of the dU-DNAzyme walker; and the effects of DTT on track strand stability on the AuNP surface (PDF)

AUTHOR INFORMATION

Corresponding Authors

Hongquan Zhang − *Division of Analytical and Environmental Toxicology, Department of Laboratory Medicine and Pathology, Faculty of Medicine and Dentistry, University of Alberta, Edmonton, Alberta T6G 2G3, Canada;*

ⓘ orcid.org/0000-0003-1088-9862; Email: hongquan@ualberta.ca

X. Chris Le − *Division of Analytical and Environmental Toxicology, Department of Laboratory Medicine and Pathology, Faculty of Medicine and Dentistry, University of Alberta, Edmonton, Alberta T6G 2G3, Canada;* ⓘ orcid.org/0000-0002-7690-6701; Email: xc.le@ualberta.ca

Authors

Jeffrey Tao − *Division of Analytical and Environmental Toxicology, Department of Laboratory Medicine and Pathology, Faculty of Medicine and Dentistry, University of Alberta, Edmonton, Alberta T6G 2G3, Canada;* ⓘ orcid.org/0000-0001-5526-8133

Michael Weinfeld − *Division of Experimental Oncology, Department of Oncology, Faculty of Medicine and Dentistry, University of Alberta, Cross Cancer Institute, Edmonton, Alberta T6G 1Z2, Canada;* ⓘ orcid.org/0000-0002-8773-1425

Complete contact information is available at:
https://pubs.acs.org/10.1021/acsmeasuresciau.4c00011

Author Contributions

The manuscript was written through contributions of all authors. All authors have given approval to the final version of the manuscript. CRediT: **Jeffrey Tao** data curation, formal analysis, investigation, methodology, validation, visualization, writing-original draft, writing-review & editing; **Hongquan Zhang** conceptualization, project administration, resources, supervision, writing-review & editing; **Michael Weinfeld** formal analysis, resources, supervision, writing-review & editing; **X. Chris Le** conceptualization, formal analysis, funding acquisition, project administration, resources, supervision, writing-original draft, writing-review & editing.

Notes

The authors declare no competing financial interest.

■ REFERENCES

(1) D'Errico, M.; Parlanti, E.; Pascucci, B.; Fortini, P.; Baccarini, S.; Simonelli, V.; Dogliotti, E. Single Nucleotide Polymorphisms in DNA Glycosylases: From Function to Disease. *Free Radic Biol. Med.* **2017**, *107*, 278−291.

(2) Mancuso, P.; Tricarico, R.; Bhattacharjee, V.; Cosentino, L.; Kadariya, Y.; Jelinek, J.; Nicolas, E.; Einarson, M.; Beeharry, N.; Devarajan, K.; Katz, R. A.; Dorjsuren, D. G.; Sun, H.; Simeonov, A.; Giordano, A.; Testa, J. R.; Davidson, G.; Davidson, I.; Larue, L.; Sobol, R. W.; Yen, T. J.; Bellacosa, A. Thymine DNA Glycosylase as a Novel Target for Melanoma. *Oncogene* **2019**, *38* (19), 3710−3728.

(3) Yun, S. J.; Ha, Y. S.; Chae, Y.; Kim, J. S.; Kim, I. Y.; Kim, W. J. The HOGG1Mutant Genotype Is Associated with Prostate Cancer Susceptibility and Aggressive Clinicopathological Characteristics in the Korean Population. *Annals of Oncology* **2012**, *23* (2), 401−405.

(4) Wu, D.; Zhang, G.; Ma, J.; Wu, H.; Xiong, J.; Huang, X.; Tian, Y.; Deng, T.; Han, X.; Sun, X.; Xiang, T.; Yu, X.; Jiang, X.

Upregulation of Nei-Like DNA Glycosylase 3 Predicts Poor Prognosis in Hepatocellular Carcinoma. *J. Oncol* **2021**, *2021*, 1−11.

(5) Pilo, J.; García-Flores, L. A.; Clemente-Postigo, M.; Arranz-Salas, I.; Alcaide, J.; Ramos-Fernandez, M.; Lozano, J.; Boughanem, H.; Kompella, P.; Macías-González, M. 8-Oxoguanine DNA Glycosylase 1 Upregulation as a Risk Factor for Obesity and Colorectal Cancer. *Int. J. Mol. Sci.* **2023**, *24* (6), 5488.

(6) Hans, F.; Senarisoy, M.; Bhaskar Naidu, C.; Timmins, J. Focus on DNA Glycosylases—A Set of Tightly Regulated Enzymes with a High Potential as Anticancer Drug Targets. *Int. J. Mol. Sci.* **2020**, *21* (23), 9226.

(7) Weeks, L. D.; Fu, P.; Gerson, S. L. Uracil-DNA Glycosylase Expression Determines Human Lung Cancer Cell Sensitivity to Pemetrexed. *Mol. Cancer Ther* **2013**, *12* (10), 2248−2260.

(8) Zhang, S.; He, L.; Dai, N.; Guan, W.; Shan, J.; Yang, X.; Zhong, Z.; Qing, Y.; Jin, F.; Chen, C.; Yang, Y.; Wang, H.; Baugh, L.; Tell, G.; Wilson, D. M.; Li, M.; Wang, D. Serum APE1 as a Predictive Marker for Platinum-Based Chemotherapy of Non-Small Cell Lung Cancer Patients. *Oncotarget* **2016**, *7* (47), 77482−77494.

(9) Grundy, G. J.; Parsons, J. L. Base Excision Repair and Its Implications to Cancer Therapy. *Essays Biochem* **2020**, *64* (5), 831−843.

(10) Baquero, J. M.; Benítez-Buelga, C.; Rajagopal, V.; Zhenjun, Z.; Torres-Ruiz, R.; Müller, S.; Hanna, B. M. F.; Loseva, O.; Wallner, O.; Michel, M.; Rodríguez-Perales, S.; Gad, H.; Visnes, T.; Helleday, T.; Benítez, J.; Osorio, A. Small Molecule Inhibitor of OGG1 Blocks Oxidative DNA Damage Repair at Telomeres and Potentiates Methotrexate Anticancer Effects. *Sci. Rep* **2021**, *11* (1), 3490.

(11) Visnes, T.; Benítez-Buelga, C.; Cázares-Körner, A.; Sanjiv, K.; Hanna, B. M. F.; Mortusewicz, O.; Rajagopal, V.; Albers, J. J.; Hagey, D. W.; Bekkhus, T.; Eshtad, S.; Baquero, J. M.; Masuyer, G.; Wallner, O.; Müller, S.; Pham, T.; Göktürk, C.; Rasti, A.; Suman, S.; Torres-Ruiz, R.; Sarno, A.; Wiita, E.; Homan, E. J.; Karsten, S.; Marimuthu, K.; Michel, M.; Koolmeister, T.; Scobie, M.; Loseva, O.; Almlöf, I.; Unterlass, J. E.; Pettke, A.; Boström, J.; Pandey, M.; Gad, H.; Herr, P.; Jemth, A.-S.; El Andaloussi, S.; Kalderén, C.; Rodriguez-Perales, S.; Benítez, J.; Krokan, H. E.; Altun, M.; Stenmark, P.; Berglund, U. W.; Helleday, T. Targeting OGG1 Arrests Cancer Cell Proliferation by Inducing Replication Stress. *Nucleic Acids Res.* **2020**, *48* (21), 12234−12251.

(12) Kreklau, E. L. A Novel Fluorometric Oligonucleotide Assay to Measure O 6-Methylguanine DNA Methyltransferase, Methylpurine DNA Glycosylase, 8-Oxoguanine DNA Glycosylase and Abasic Endonuclease Activities: DNA Repair Status in Human Breast Carcinoma Cells Overexpressing Methylpurine DNA Glycosylase. *Nucleic Acids Res.* **2001**, *29* (12), 2558−2566.

(13) Sudina, A. E.; Volkov, E. M.; Oretskaya, T. S.; Degtyarev, S. K.; Gonchar, D. A.; Kubareva, E. A. An Express Method for Testing the Activity of a Repair Enzyme, Uracil-DNA-Glycosylase. *Russ. J. Bioorg. Chem.* **2000**, *26* (6), 398−402.

(14) Xia, L.; O'Connor, T. R. DNA Glycosylase Activity Assay Based on Streptavidin Paramagnetic Bead Substrate Capture. *Anal. Biochem.* **2001**, *298* (2), 322−326.

(15) García-Ortiz, M.-V.; Ariza, R. R.; Roldán-Arjona, T. A Chemiluminescent Method for the Detection of DNA Glycosylase/Lyase Activity. *Anal. Biochem.* **2001**, *298* (1), 127−129.

(16) Ouyang, Y.; Liu, Y.; Deng, Y.; He, H.; Huang, J.; Ma, C.; Wang, K. Recent Advances in Biosensor for DNA Glycosylase Activity Detection. *Talanta* **2022**, *239*, No. 123144.

(17) Wang, L.; Zhang, H.; Chen, W.; Chen, H.; Xiao, J.; Chen, X. Recent Advances in DNA Glycosylase Assays. *Chin. Chem. Lett.* **2022**, *33* (8), 3603−3612.

(18) Wang, L.; Liu, Q.; Ma, F.; Zhang, C. Target-Responsive DNAzyme Probes for Luminescence Detection and Imaging of DNA-Modifying Enzymes. *TrAC Trends in Analytical Chemistry* **2023**, *167*, No. 117270.

(19) Chen, F.; Bai, M.; Cao, K.; Zhao, Y.; Wei, J.; Zhao, Y. Fabricating MnO $_2$ Nanozymes as Intracellular Catalytic DNA Circuit

Generators for Versatile Imaging of Base-Excision Repair in Living Cells. *Adv. Funct Mater.* **2017**, 27 (45), No. 1702748.

(20) Dong, K.; Shu, W.; Zhang, J.; Cheng, S.; Zhang, J.; Zhao, R.; Hua, T.; Zhang, W.; Wang, H. Ultra-Sensitive Biosensor Based on CRISPR-Cas12a and Endo IV Coupled DNA Hybridization Reaction for Uracil DNA Glycosylase Detection and Intracellular Imaging. *Biosens Bioelectron* **2023**, 226, No. 115118.

(21) Song, X.; Ding, Q.; Zhang, J.; Sun, R.; Yin, L.; Wei, W.; Pu, Y.; Liu, S. Smart Catalyzed Hairpin Assembly-Induced DNAzyme Nanosystem for Intracellular UDG Imaging. *Anal. Chem.* **2021**, 93 (40), 13687−13693.

(22) Zhang, Q.; Li, C.; Ma, F.; Luo, X.; Zhang, C. Catalytic Single-Molecule Förster Resonance Energy Transfer Biosensor for Uracil-DNA Glycosylase Detection and Cellular Imaging. *Biosens Bioelectron* **2022**, 213, No. 114447.

(23) Seferos, D. S.; Prigodich, A. E.; Giljohann, D. A.; Patel, P. C.; Mirkin, C. A. Polyvalent DNA Nanoparticle Conjugates Stabilize Nucleic Acids. *Nano Lett.* **2009**, 9 (1), 308−311.

(24) Seferos, D. S.; Giljohann, D. A.; Hill, H. D.; Prigodich, A. E.; Mirkin, C. A. Nano-Flares: Probes for Transfection and MRNA Detection in Living Cells. *J. Am. Chem. Soc.* **2007**, 129 (50), 15477−15479.

(25) Choi, C. H. J.; Hao, L.; Narayan, S. P.; Auyeung, E.; Mirkin, C. A. Mechanism for the Endocytosis of Spherical Nucleic Acid Nanoparticle Conjugates. *Proc. Natl. Acad. Sci. U. S. A.* **2013**, 110 (19), 7625−7630.

(26) Patel, P. C.; Giljohann, D. A.; Daniel, W. L.; Zheng, D.; Prigodich, A. E.; Mirkin, C. A. Scavenger Receptors Mediate Cellular Uptake of Polyvalent Oligonucleotide-Functionalized Gold Nanoparticles. *Bioconjug Chem.* **2010**, 21 (12), 2250−2256.

(27) Wu, X. A.; Choi, C. H. J.; Zhang, C.; Hao, L.; Mirkin, C. A. Intracellular Fate of Spherical Nucleic Acid Nanoparticle Conjugates. *J. Am. Chem. Soc.* **2014**, 136 (21), 7726−7733.

(28) Behzadi, S.; Serpooshan, V.; Tao, W.; Hamaly, M. A.; Alkawareek, M. Y.; Dreaden, E. C.; Brown, D.; Alkilany, A. M.; Farokhzad, O. C.; Mahmoudi, M. Cellular Uptake of Nanoparticles: Journey inside the Cell. *Chem. Soc. Rev.* **2017**, 46 (14), 4218−4244.

(29) Narayan, S. P.; Choi, C. H. J.; Hao, L.; Calabrese, C. M.; Auyeung, E.; Zhang, C.; Goor, O. J. G. M.; Mirkin, C. A. The Sequence-Specific Cellular Uptake of Spherical Nucleic Acid Nanoparticle Conjugates. *Small* **2015**, 11 (33), 4173−4182.

(30) Tao, J.; Zhang, H.; Weinfeld, M.; Le, X. C. Development of a DNAzyme Walker for the Detection of APE1 in Living Cancer Cells. *Anal. Chem.* **2023**, 95 (40), 14990−14997.

(31) Bellamy, S. R. W.; Krusong, K.; Baldwin, G. S. A Rapid Reaction Analysis of Uracil DNA Glycosylase Indicates an Active Mechanism of Base Flipping. *Nucleic Acids Res.* **2007**, 35 (5), 1478−1487.

(32) Stivers, J. T.; Pankiewicz, K. W.; Watanabe, K. A. Kinetic Mechanism of Damage Site Recognition and Uracil Flipping by *Escherichia Coli* Uracil DNA Glycosylase. *Biochemistry* **1999**, 38 (3), 952−963.

(33) Masaoka, A.; Matsubara, M.; Hasegawa, R.; Tanaka, T.; Kurisu, S.; Terato, H.; Ohyama, Y.; Karino, N.; Matsuda, A.; Ide, H. Mammalian 5-Formyluracil−DNA Glycosylase. 2. Role of SMUG1 Uracil−DNA Glycosylase in Repair of 5-Formyluracil and Other Oxidized and Deaminated Base Lesions. *Biochemistry* **2003**, 42 (17), 5003−5012.

(34) Kavli, B.; Sundheim, O.; Akbari, M.; Otterlei, M.; Nilsen, H.; Skorpen, F.; Aas, P. A.; Hagen, L.; Krokan, H. E.; Slupphaug, G. HUNG2 Is the Major Repair Enzyme for Removal of Uracil from U:A Matches, U:G Mismatches, and U in Single-Stranded DNA, with HSMUG1 as a Broad Specificity Backup. *J. Biol. Chem.* **2002**, 277 (42), 39926−39936.

(35) O'Neill, R. J.; Vorobeva, O. V.; Shahbakhti, H.; Zmuda, E.; Bhagwat, A. S.; Baldwin, G. S. Mismatch Uracil Glycosylase from *Escherichia coli*: A General Mismatch or a Specific DNA Glycosylase? *J. Biol. Chem.* **2003**, 278 (23), 20526−20532.

(36) Schormann, N.; Ricciardi, R.; Chattopadhyay, D. Uracil-DNA Glycosylases—Structural and Functional Perspectives on an Essential Family of DNA Repair Enzymes. *Protein Sci.* **2014**, 23 (12), 1667−1685.

(37) Slupphaug, G.; Eftedal, I.; Kavli, B.; Bharati, S.; Helle, N. M.; Haug, T.; Levine, D. W.; Krokan, H. E. Properties of a Recombinant Human Uracil-DNA Glycosylase from the UNG Gene and Evidence That UNG Encodes the Major Uracil-DNA Glycosylase. *Biochemistry* **1995**, 34 (1), 128−138.

(38) Mosbaugh, D. W.; Bennett, S. E. Uracil-Excision DNA Repair. *Prog. Nucleic Acid Res. Mol. Biol.* **1994**, 48, 315−370.

(39) Mol, C. D.; Arvai, A. S.; Slupphaug, G.; Kavli, B.; Alseth, I.; Krokan, H. E.; Tainer, J. A. Crystal Structure and Mutational Analysis of Human Uracil-DNA Glycosylase: Structural Basis for Specificity and Catalysis. *Cell* **1995**, 80 (6), 869−878.

(40) Krokan, H.; Urs Wittwer, C. Uracil DNA-Glycosylase from HeLa Cells: General Properties, Substrate Specificity and Effect of Uracil Analogs. *Nucleic Acids Res.* **1981**, 9 (11), 2599−2614.

(41) Savva, R.; McAuley-Hecht, K.; Brown, T.; Pearl, L. The Structural Basis of Specific Base-Excision Repair by Uracil−DNA Glycosylase. *Nature* **1995**, 373 (6514), 487−493.

(42) Luo, N.; Mehler, E.; Osman, R. Specificity and Catalysis of Uracil DNA Glycosylase. A Molecular Dynamics Study of Reactant and Product Complexes with DNA. *Biochemistry* **1999**, 38 (29), 9209−9220.

(43) Drohat, A. C.; Jagadeesh, J.; Ferguson, E.; Stivers, J. T. Role of Electrophilic and General Base Catalysis in the Mechanism of Escherichia Coli Uracil DNA Glycosylase. *Biochemistry* **1999**, 38 (37), 11866−11875.

(44) Li, C.; Long, Y.; Liu, B.; Xiang, D.; Zhu, H. Real Time Monitoring Uracil Excision Using Uracil-Containing Molecular Beacons. *Anal. Chim. Acta* **2014**, 819, 71−77.

(45) Maher, R. L.; Bloom, L. B. Pre-Steady-State Kinetic Characterization of the AP Endonuclease Activity of Human AP Endonuclease 1. *J. Biol. Chem.* **2007**, 282 (42), 30577−30585.

(46) Schermerhorn, K. M.; Delaney, S. Transient-State Kinetics of Apurinic/Apyrimidinic (AP) Endonuclease 1 Acting on an Authentic AP Site and Commonly Used Substrate Analogs: The Effect of Diverse Metal Ions and Base Mismatches. *Biochemistry* **2013**, 52 (43), 7669−7677.

(47) Kladova, O. A.; Alekseeva, I. V.; Saparbaev, M.; Fedorova, O. S.; Kuznetsov, N. A. Modulation of the Apurinic/Apyrimidinic Endonuclease Activity of Human APE1 and of Its Natural Polymorphic Variants by Base Excision Repair Proteins. *Int. J. Mol. Sci.* **2020**, 21 (19), 7147.

(48) Baldwin, M. R.; O'Brien, P. J. Human AP Endonuclease 1 Stimulates Multiple-Turnover Base Excision by Alkyladenine DNA Glycosylase. *Biochemistry* **2009**, 48 (25), 6022−6033.

(49) Kladova, O. A.; Bazlekowa-Karaban, M.; Baconnais, S.; Piétrement, O.; Ishchenko, A. A.; Matkarimov, B. T.; Iakovlev, D. A.; Vasenko, A.; Fedorova, O. S.; Le Cam, E.; Tudek, B.; Kuznetsov, N. A.; Saparbaev, M. The Role of the N-Terminal Domain of Human Apurinic/Apyrimidinic Endonuclease 1, APE1, in DNA Glycosylase Stimulation. *DNA Repair (Amst)* **2018**, 64, 10−25.

(50) Nilsen, H.; Haushalter, K. A.; Robins, P.; Barnes, D. E.; Verdine, G. L.; Lindahl, T. Excision of Deaminated Cytosine from the Vertebrate Genome: Role of the SMUG1 Uracil-DNA Glycosylase. *EMBO J.* **2001**, 20 (15), 4278−4286.

(51) Hölz, K.; Pavlic, A.; Lietard, J.; Somoza, M. M. Specificity and Efficiency of the Uracil DNA Glycosylase-Mediated Strand Cleavage Surveyed on Large Sequence Libraries. *Sci. Rep* **2019**, 9 (1), 17822.

(52) Eftedal, I.; Guddal, P. H.; Slupphaug, G.; Volden, G.; Krokan, H. E. Consensus Sequences for Good and Poor Removal of Uracil from Double Stranded DNA by Uracil-DNA Glycosylase. *Nucleic Acids Res.* **1993**, 21 (9), 2095−2101.

(53) Pettersen, H. S.; Sundheim, O.; Gilljam, K. M.; Slupphaug, G.; Krokan, H. E.; Kavli, B. Uracil−DNA Glycosylases SMUG1 and UNG2 Coordinate the Initial Steps of Base Excision Repair by Distinct Mechanisms. *Nucleic Acids Res.* **2007**, 35 (12), 3879−3892.

(54) Haushalter, K. A.; Todd Stukenberg, P.; Kirschner, M. W.; Verdine, G. L. Identification of a New Uracil-DNA Glycosylase Family by Expression Cloning Using Synthetic Inhibitors. *Curr. Biol.* **1999**, *9* (4), 174−185.

(55) Acharya, N.; Roy, S.; Varshney, U. Mutational Analysis of the Uracil DNA Glycosylase Inhibitor Protein and Its Interaction with Escherichia Coli Uracil DNA Glycosylase. *J. Mol. Biol.* **2002**, *321* (4), 579−590.

(56) Bennett, S. E.; Mosbaugh, D. W. Characterization of the Escherichia Coli Uracil-DNA Glycosylase.Inhibitor Protein Complex. *J. Biol. Chem.* **1992**, *267* (31), 22512−22521.

(57) Miroshnikova, A. D.; Kuznetsova, A. A.; Vorobjev, Y. N.; Kuznetsov, N. A.; Fedorova, O. S. Effects of Mono- and Divalent Metal Ions on DNA Binding and Catalysis of Human Apurinic/ Apyrimidinic Endonuclease 1. *Mol. Biosyst* **2016**, *12* (5), 1527−1539.

(58) Alexeeva, M.; Moen, M. N.; Xu, X. M.; Rasmussen, A.; Leiros, I.; Kirpekar, F.; Klungland, A.; Alsøe, L.; Nilsen, H.; Bjelland, S. Intrinsic Strand-Incision Activity of Human UNG: Implications for Nick Generation in Immunoglobulin Gene Diversification. *Front. Immunol.* **2021**, *12*, No. 762032.

(59) Doseth, B.; Visnes, T.; Wallenius, A.; Ericsson, I.; Sarno, A.; Pettersen, H. S.; Flatberg, A.; Catterall, T.; Slupphaug, G.; Krokan, H. E.; Kavli, B. Uracil-DNA Glycosylase in Base Excision Repair and Adaptive Immunity: Species Differences between Man and Mouse. *J. Biol. Chem.* **2011**, *286* (19), 16669−16680.

(60) Waters, T. R.; Swann, P. F. Kinetics of the Action of Thymine DNA Glycosylase. *J. Biol. Chem.* **1998**, *273* (32), 20007−20014.

(61) Mol, C. D.; Arvai, A. S.; Sanderson, R. J.; Slupphaug, G.; Kavli, B.; Krokan, H. E.; Mosbaugh, D. W.; Tainer, J. A. Crystal Structure of Human Uracil-DNA Glycosylase in Complex with a Protein Inhibitor: Protein Mimicry of DNA. *Cell* **1995**, *82* (5), 701−708.

(62) Savva, R.; Pearl, L. H. Nucleotide Mimicry in the Crystal Structure of the Uracil-DNA Glycosylase−Uracil Glycosylase Inhibitor Protein Complex. *Nat. Struct Mol. Biol.* **1995**, *2* (9), 752− 757.

(63) Gallinari, P.; Jiricny, J. A New Class of Uracil-DNA Glycosylases Related to Human Thymine-DNA Glycosylase. *Nature* **1996**, *383* (6602), 735−738.

(64) Bulgar, A. D.; Weeks, L. D.; Miao, Y.; Yang, S.; Xu, Y.; Guo, C.; Markowitz, S.; Oleinick, N.; Gerson, S. L.; Liu, L. Removal of Uracil by Uracil DNA Glycosylase Limits Pemetrexed Cytotoxicity: Overriding the Limit with Methoxyamine to Inhibit Base Excision Repair. *Cell Death Dis* **2012**, *3* (1), e252−e252.

(65) Jiang, R.; Shen, H.; Piao, Y.-J. The Morphometrical Analysis on the Ultrastructure of A549 Cells. *Rom. J. Morphol. Embryol.* **2010**, *51* (4), 663−667.

(66) Park, J.; Evangelopoulos, M.; Vasher, M. K.; Kudruk, S.; Ramani, N.; Mayer, V.; Solivan, A. C.; Lee, A.; Mirkin, C. A. Enhancing Endosomal Escape and Gene Regulation Activity for Spherical Nucleic Acids. *Small* **2024**, *20*, No. e2306902.

(67) Tsoi, K. M.; MacParland, S. A.; Ma, X.-Z.; Spetzler, V. N.; Echeverri, J.; Ouyang, B.; Fadel, S. M.; Sykes, E. A.; Goldaracena, N.; Kaths, J. M.; Conneely, J. B.; Alman, B. A.; Selzner, M.; Ostrowski, M. A.; Adeyi, O. A.; Zilman, A.; McGilvray, I. D.; Chan, W. C. W. Mechanism of Hard-Nanomaterial Clearance by the Liver. *Nat. Mater.* **2016**, *15* (11), 1212−1221.